JMEPEG (2008) 17:254–259
DOI: 10.1007/s11665-007-9135-y

1059-9495/$19.00

Size and Shape Effects for Gamma Prime in Alloy 738

Charles Hays

(Submitted January 9, 2007; in revised form May 18, 2007)

Cast IN-738 and wrought Inconel 738 are generic applications for most metallurgical designers of gas turbine blades in the Power Generation Industry on a worldwide basis... Particularly, where first stage buckets are concerned. This is the case because both alloy types exhibit outstanding creep and stress rupture properties to provide an extended service period in a harsh environment. Typically, Alloy 738 is fired in the turbine at 1970 °F (1074 °C) which is about 0.9T_m where T_m represents the melting temperature... A very demanding service temperature, indeed. Furthermore, Alloy 738 is expected to endure this high temperature for a duration of 26,000 h at base load before being retired (R) or replaced (R′) or reused (R″) issues are ever considered. When these three (3) problems (R-R′-R″) are brought before a given Materials Review Board for appropriate debate, many pro and con arguments are always evident because (1) Gas turbine blades are not inexpensive and (2) The threat of field failures with possible product liability litigation is of maximum interest to all gas turbine repair shop personnel. The intent of this paper is show how gamma prime precipitate particles can be better examined and more efficiently evaluated using a new characterization method. This research is offered as a contribution to the sum of total knowledge.

Keywords annealing/aging, athermal transformation, coring, dendrites, diffusion controlled growth, extrusion, hardness and quantitative metallography, IN-738, Inconel 738, interstitial controlled growth, microcracking, overaging, point counting, replacement, retirement, reusage, segregation, slowcooling, thermal transformation, waterquenched

1. Introduction

Some confusion still exists about the different designations for Alloy 738. "IN-738" refers to cast turbine blade material and "INCONEL 738" describes wrought products, either extruded or forged. Clarence G. Bieber and co-workers discovered INCONEL 738 alloy in about 1970 while being employed by the International Nickel Company of New York, NY (Ref 1). Subsequent development of Bieber's alloy led to considerable success as an investment-cast alloy, IN-738. Widespread usage of IN-738 extended through 2004 because of its attractive fatigue and creep strength properties. In December of 2004, Sheimbob and co-workers at EXTEX reverted from IN-738 back to the original INCONEL 738 using a forged turbine blade (Ref 2). The work at EXTEX more than doubled the service life over that for the original equipment manufacturer (OEM) which used only investment-cast turbine blades. Sheimbob's breakthrough discovery also revealed that a CNC-machined forging yielded other improvements; e.g., consider these advantages... A 4% increase in power output with a 1.5% reduction in specific fuel consumption for a cost savings of about 40%. Unfortunately, these new EXTEX observations were restricted to small turbine blades, not large ones... Their work concentrated on blades for helicopters and an aero-derivative engine that was designed by ROLLS-ROYCE. But, Sheimbob's work more than justifies a wrought approach for all sizes of turbine blades.

At this time, the marketplace for large industrial gas turbine blades offers only investment-cast blades of IN-738 alloy with some recent enhancements of better casting techniques and an improved understanding of aging kinetics (Ref 3) or carbide decomposition effects (Ref 4). Certainly, better performance results do vindicate the use of wrought turbine blades for large GE Frame 6 or Frame 7 units at the various FAA-approved repair stations. The goal of this research is to use extrusions (not forgings) to generate an improved turbine blade which contains a lower interstitial content with controlled additives for the avoidance of deleterious phases exhibiting these advantages... No microcracks, no continuous carbide networks, and an equilibrium structure using the appropriate CNC/EDM shaping processes. This paper is dedicated to the process of extrusion with compatible thermal processing to achieve important size and shape effects for gamma prime in this apparent rebirth of Bieber's old INCONEL 738 alloy.

2. Materials

The materials used in this investigation involved primarily ingot-cast INCONEL 738 in the following conditions: cast, annealed, annealed + aged and extruded. Investment-cast turbine blade samples of IN-738 were examined for comparison purposes; i.e., to study the over-aged state for this alloy chemistry. This paper describes portions of a work-in-progress. Previously, the mechanical properties of ingot-cast 738 were reported (Ref 5). This particular paper deals with observed differences in size and shape effects for gamma prime particles as affected by different processing variables. The third and final paper of this series will be dedicated to differences between investment-cast blades vs. ingot-cast blades of alloy 738.

Charles Hays, Hays Metallurgical Engineering Corp., PO Box 3250, Pearland, TX 77588. Contact e-mail: haysmet@aol.com.

All observations taken from actual turbine blades were extracted from the airfoil regions looking only at the transverse direction. Ingot-cast specimens and their associated derivatives (e.g., extruded material) were sectioned to reveal both the longitudinal and transverse orientations. Regarding this current research, the materials sponsor was BTEC Turbines, Ltd. of Houston, TX. All examinations and opinions represent intellectual property belonging to the author. This is to say that this characterization research was funded by Hays Metallurgical of Pearland, TX. A provisional patent (Ref 6) has already been issued to the author so, a "patent pending" status currently applies.

3. Methods

Investment-cast and ingot-cast samples were each sectioned into specimens using diamond wafering blades and a small wire electrical discharge machining (EDM) method. Characterization of microstructure was achieved by using properly prepared specimens as obtained from the ABRAPOL and SYNTRON appliances. Perhaps, the greatest challenge to the study of these polished specimens involved problems concerning the electro-etching of this alloy. The most popular electrolytic etchant of 10% chromic acid (Aq.) caused excessively thick layers of an anodization product to form. And, the EM-4 electro-etchant proposed by Petzow (Ref 7) was overly active to the degree that these specimens were over-etched in less than one (1) second of exposure to voltage across the cell. For this investigation, a modified "EM-400" solution was developed using film thickness as a monitor so that water content of the bath could be correctly adjusted for proper contrast allowing an extended exposure time. The solution to this problem required an addition of 475-mL of spring water to Petzow's EM-4 reagent. Even with the addition of more water, etching times were brief (one-to-three seconds) with 3-V DC using the BUEHLER ELECTROMET ETCHER. Best results occur when the bath is stored in a refrigerator and used only in the cold condition.

Optical photomicrographs were created using only digital camera technology. Secondary electron imaging (SEI) provided the scanning electron microscope (SEM) results. Quantitative metallography involved the development of a new point counting procedure and associated statistical studies were applied; viz., correlation, regression and severity determinations. Finally, hardness studies were undertaken using the scientific approach that is generally reserved for the calibration of Rockwell C hardness blocks.

4. Discussion

Figure 1 is an optical photomicrograph of a blade sample created by the investment-cast process. This specific specimen represents all that is imperfect with a cast turbine blade... Coring, porosity, degenerated carbides, a nonequilibrium microstructure, duplex-sized dendrites and microcracking. This paper attempts to circumvent all highly controversial arguments about "favorites" for either cast or wrought industrial gas turbine blades. Instead, this work is dedicated to a better understanding of how to properly evaluate blade microstructure.

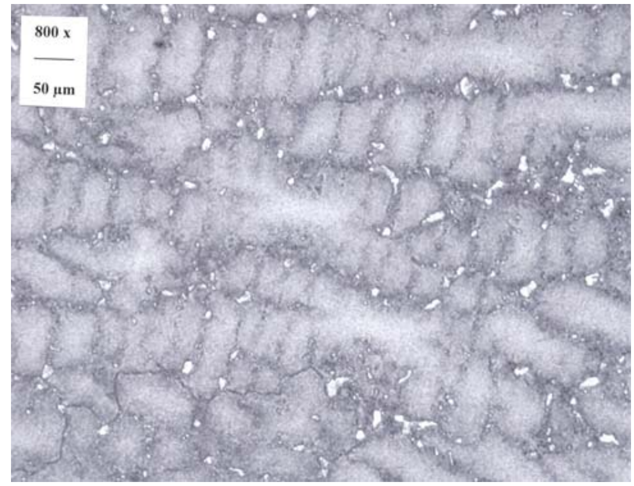

Fig. 1 Typical microstructure for an investment-cast turbine blade at 800×

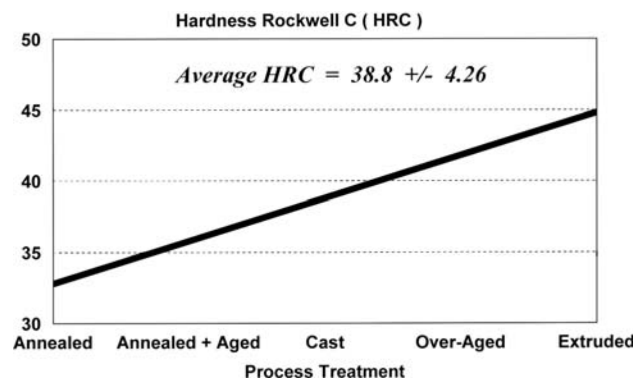

Fig. 2 Variation of hardness for the different conditions of state

Figure 2 is an engineering graph that considers Rockwell C hardness data for the different conditions that were evaluated; annealed, annealed + aged, cast, over-aged and extruded. The resulting trend curve makes the statement that this alloy system gains strength by a simple mechanism... The more gamma prime that can be close-packed into an austenitic matrix is the driver for both hardness and strength. Longer aging times at the appropriate aging temperature do not cause softening for this alloy. This is to make the point that Preston zones (Ref 8) do not here apply. However, it must also be stated that, because this variance in hardness is so small, hardness testing must be done using only statistical sampling routines and calibrated equipment.

Figure 3 is taken from the best book ever written on the sole subject of superalloy microstructures (Ref 9). In her book, Madeline Durand-Charre describes the work of Grosdidier et al. (Ref 10). Grosdidier first gave the open literature an original method for evaluating size and shape effects of gamma prime in superalloys. Certainly, that classic contribution deserves some additional discussion because Grosdidier and co-workers actually discovered a method to evaluate retirement (R), replacement (R′) and reuse (R″) for turbine blades.

According to Grosdidier, a precipitated gamma prime particle whose shape is spheroidal, cuboidal or an ogdoadical-lydiced cube is controlled by interfacial growth. Here, the

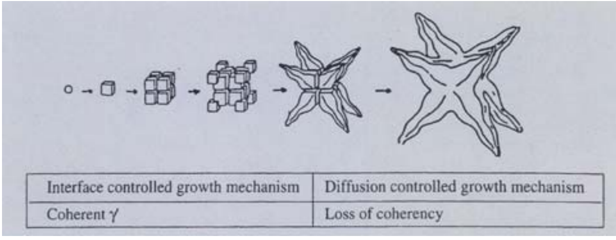

Fig. 3 Size and shape theory according to Grosdidier et al. (Ref 10) from Durand-Charre (Ref 9)

Fig. 4 Typical microstructure for the fully wrought condition at 5000×

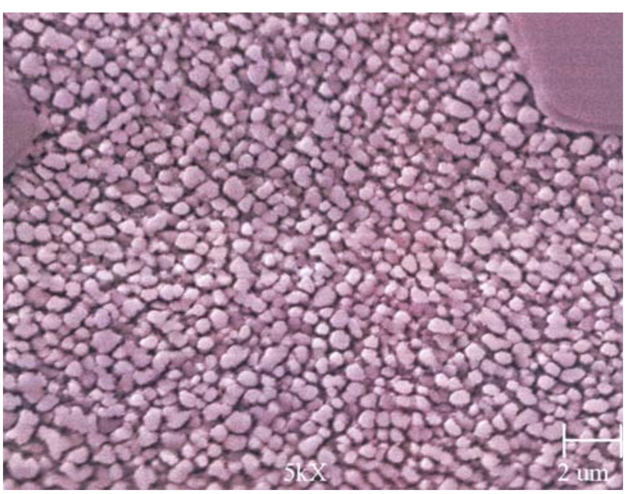

Fig. 5 Typical microstructure for an anti-mu heat treatment at 5000×

gamma prime is coherent with it's austenitic matrix and retirement (R) cannot be an issue.

However, if the gamma prime precipitate is observed as becoming that of a dendritic form where the ogdoadicallydiced cube forms either octodendrites or dendrites, the situation is one of diffusion controlled growth and a distinct loss in coherency then exists. Accordingly, technicians look for ‘‘ears’’ on their gamma prime shapes and, if ‘‘ears’’ exist, turbine blades are almost always replaced (R′). ‘‘Ears’’ alone do not justify a proper decision by a technician of that sort. In defense of that person, one could ask, ‘‘What does an eight-sided dendrite look like after being sectioned in an infinite number of orientations?’’ Clearly a better, more simplistic experimental method is badly needed and this paper attempts to address those needs and their associated priorities.

Consider an exemplar electron micrograph at a magnification of 5000×. For a given 5 in. × 7 in. (127 mm × 178 mm) photograph, draw five 1 in. (25.4 mm) reference squares at random. Draw the hypotenuse for each of these five reference squares which become line length (L). The appropriate equation is given as follows:

$$D = L/N \quad \text{(Eq 1)}$$

where D = the average gamma prime precipitate size, L = the reference line length at 5000× (1.414 in. or 35.9 mm) and N = the number of intercepts that gamma prime particles make with respect to the reference line. As a typical case, let the actual length (L_A) be (1.414) 5000 and N = 20, 24, 21, 23, 22 such that this $D = 0.3192 \pm 0.023$ μm. The variation about all observed values is called severity (S) where the (Standard deviation is divided by the arithmetic mean) times 100 or, in this example, S = 7.2%. In this manner, a quantitative result can be obtained for dealing with the more controversial issue of an octodendritic shape vs. a dendritic shape. And, this new procedure can be used across the entire spectrum of all gamma prime sizes and shapes... Spheres, cubes, ogdoadicallydiced cubes, octodendrites and dendrites.

Figure 4 is an electron micrograph of the fully wrought condition after extrusion. Here, the gamma prime morphology is one of entirely submicroscopic spheres where sub-microscopic is defined as less than 1 μm. Its dispersion throughout the austenitic matrix is both uniform and continuous. Since the prevalent shape is very small spheres, coherency with the gamma matrix applies where an interface controlled growth mechanism is dominant. In this condition and, at the magnification of 5000×, this gamma prime precipitate can be properly point-counted and, subsequently, studied on more quantitative terms. Here, three distinct grains are intersecting at almost a 120° included angle so, conversion from cast to wrought has been substantially completed. The grain boundaries for this fully wrought microstructure of INCONEL 738 contain a discontinuous array of complex carbides as (M_xC_y)... Presumed to be $M_{12}C$ after the work of Duval et al. (Ref 11). For this as-extruded specimen, the average D was determined to be 0.198 ± 0.019 μm.

Figure 5 is an electron micrograph at 5000× showing a typical structure which exists after an anti-mu thermal treatment has been applied. This special heat treatment requires two furnaces with an immediate hot transfer. One furnace is set for annealing and the second furnace is set at a temperature below which the deleterious Mu phase forms. Here, some larger spheres still remain but, primarily, numerous cuboidal shapes abound. This makes the statement that interface controlled growth is still operative where coherency yet exists. It suffices to say that, in this instance, the gamma prime particles are larger than that for the previous illustration. Here, the average D was measured at 0.348 ± 0.044 μm. Degenerative carbides are also evident... See the top right corner of this electron micrograph.

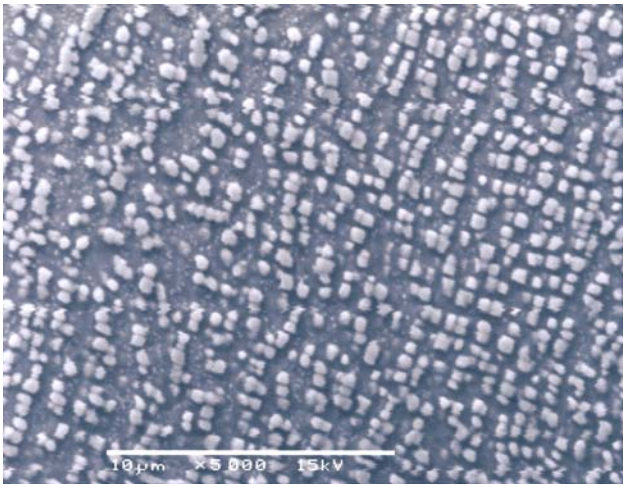

Fig. 6 Typical microstructure for a slow-cooled specimen at 5000×

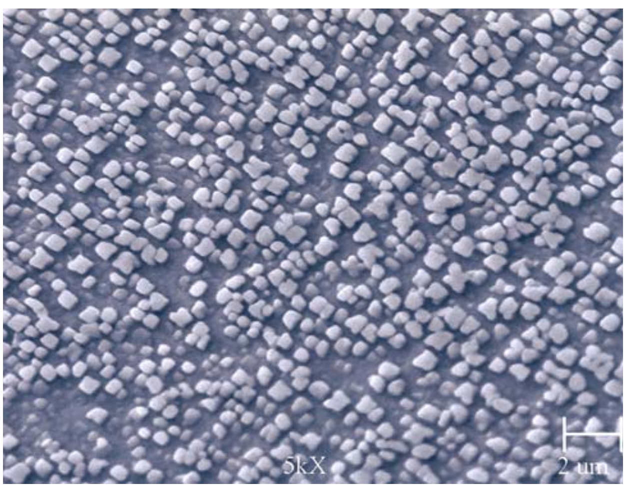

Fig. 7 Typical microstructure for the homogenized condition at 5000×

Figure 6 is an electron micrograph at 5000× revealing the results of a slow-cooling event from about $0.5T_\mathrm{m}$ to ambient. This gamma prime microstructure consists of occasional large spheres, many smaller spheres and larger cuboids. This gamma matrix offers ample space for small reforming spheres of gamma prime through the process of an interface biased growth mechanism. Accordingly, coherency with the matrix still prevails. For this sample with its associated thermal history, the average *D* was observed at $0.482 \pm 0.0.087$.

Figure 7 is an electron micrograph at 5000× depicting the homogenized condition which was water-quenched from approximately $0.6T_\mathrm{m}$ to ambient. This experiment was justified so that the microstructure at typical aging temperatures could be better understood for cross comparisons with the previous illustration (Fig. 6). Actually, these two structures (Fig. 6 vs. Fig. 7) are quite similar, except that the water-quenched sample is somewhat coarser that the slow-cooled specimen. Arguably, both micrographic fields embody the same type and form. For this condition, the average *D* was resolved at 0.498 ± 0.062.

Figure 8 is an electron micrograph at 2500× which defines an interesting problem for the turbine blade industry relating to important economic decisions about either retirement (R) or reusage (R″). This particular blade was retired by another laboratory in the Houston area because of the apparent "ears" that were observed. So, the obvious question is... Was retirement (R) a proper metallurgical decision by that technologist? A detailed re-examination by a different laboratory (HMEC) proved that this particular blade should not have been retired (R)... Instead, this blade should have been reused (R″). This is the case because extended service life was predictable on the basis that submicroscopic *D* values still remained... For example, this average *D* was computed to be 0.70 ± 0.085 μm. Reactive carbides are also here evident... See the lower left region of this microphotograph.

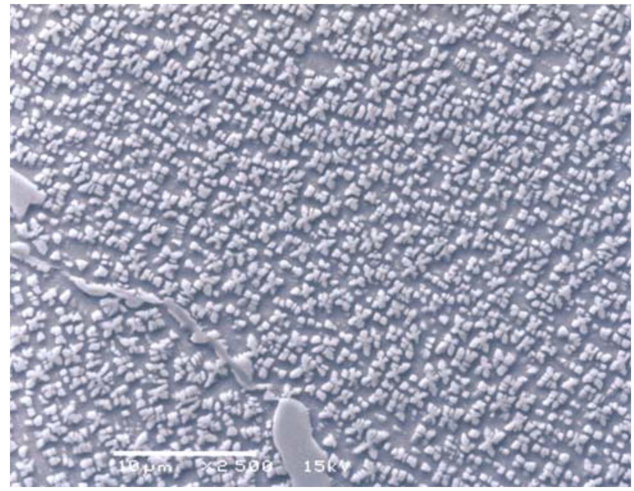

Fig. 8 Typical microstructure for a blade that was wrongfully retired at 2500×

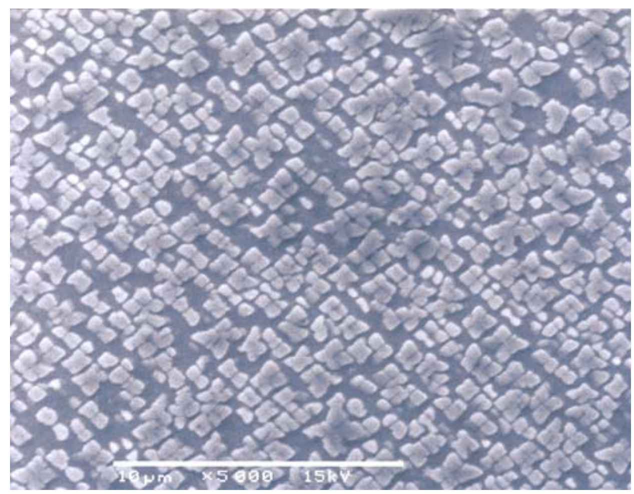

Fig. 9 Typical microstructure for a hypodendritic turbine blade at 5000×

Then, a significant other question evolves... What is the critical size for a valid retirement (R) and replacement (R′) decision? The answer to this issue is seen when two blade samples from China are properly scrutinized.

Figure 9 is an electron micrograph at 5000× where a turbine blade sample is attempting to go toward the dendritic form. As a result, this specimen condition is being driven by a diffusion

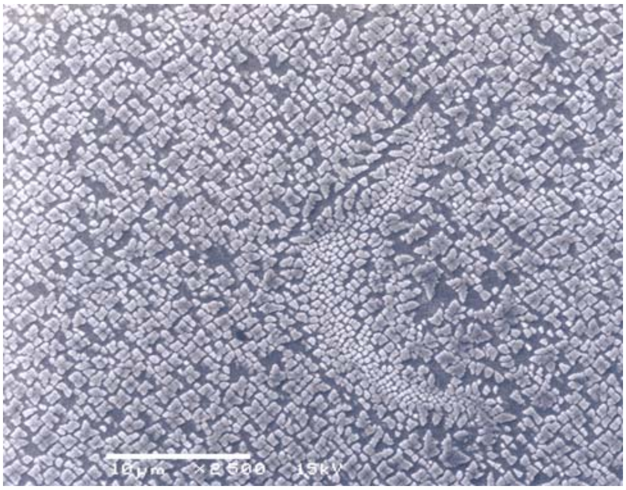

Fig. 10 Typical microstructure for a hyperdendritic turbine blade at 2500×

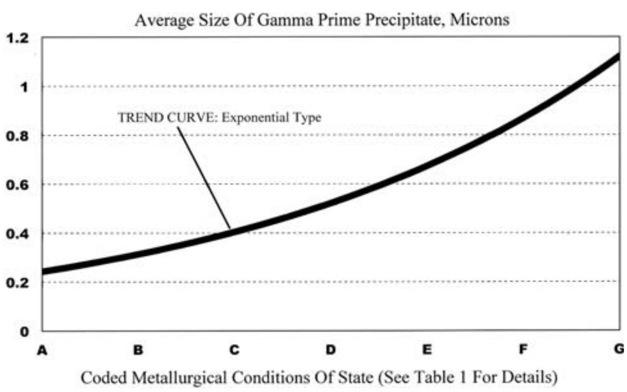

Fig. 11 Variation of gamma prime size vs. conditions of state

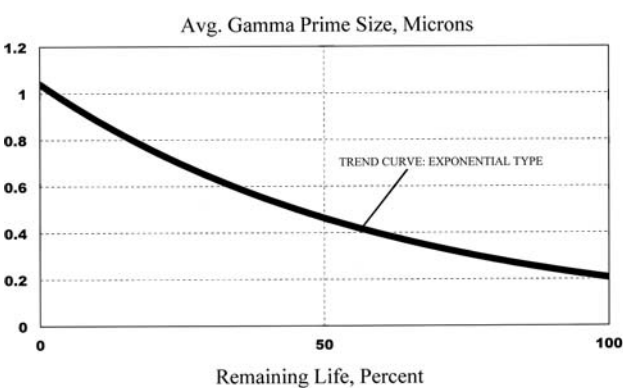

Fig. 12 Remaining life curve for Alloy 738

controlled growth mechanism. Also, large gamma prime particles are commonplace such that the average $D = 0.904 \pm 0.166$. Figure 10 is an electron micrograph at 2500× where another blade sample from China reveals even a greater tendency to become dendritic. Here, a large quasi-dendrite is being grown within an areal dimension that is greater than 400 μm^2. For this specimen, the average $D = 1.001 \pm 0.124$ μm. Both samples from China do merit a

Table 1 Reference values for experimental observations

Average gamma prime precipitate size, μm	Previous history	Associated design temperature, T/T_m
0.198 ± 0.019	(A) As-extruded	0.3[a]
0.348 ± 0.044	(B) Anti-mu treatment	0.4[a]
0.482 ± 0.087	(C) Slow-cooled	0.5[a]
0.498 ± 0.062	(D) Water-quenched	0.6[a]
0.700 ± 0.085	(E) Retired by another party	0.7[b]
0.904 ± 0.166	(F) Several over-aged	0.8[b]
1.001 ± 0.124	(G) Severely over-aged	0.9[b]

[a]In the range of 0.3-0.6T_m, these conditions hold: (1) interface controlled growth exists, (2) the gamma prime precipitate is coherent with its gamma matrix, and (3) diffusion of interstitial atoms occurs
[b]In the range of 0.7-0.9T_m, these conditions hold: (A) diffusion controlled growth applies, (B) the gamma prime precipitate is incoherent with its gamma matrix, and (C) diffusion of substitutional atoms occurs

Table 2 Reference values for remaining life predictions[a]

Observed value of D, μm	Remaining life, %	Spent life, %
0.2 = D (min)	100	0
0.3	87.5	12.5
0.4	75	25
0.5	62.5	37.5
0.6	50	50
0.7	37.5	62.5
0.8	25	75
0.9	12.5	87.5
1.0 = D (max)	0	100

[a]Based on these normalized assumptions: (1) that D (min) and D (max) serve as boundary limits and (2) That useful life exists only between the limits of 0 and 100%. In other words, it would be unsafe to use turbine blades where D is greater than 1.0 μm. Also, life beyond 100% is defined as nonexistent and too risky for reliable predictions

valid retirement (R) decision because D is microscopic as opposed to being submicroscopic. This leads to a design rule that says...

$$\text{If } D \text{ is submicroscopic } (<1\ \mu\text{m}), \text{ reuse.}$$
$$\text{If } D \text{ is microscopic } (>1\ \mu\text{m}), \text{ retire.}$$

Figure 11 is a trend curve which places all of this into a more meaningful perspective. If D is plotted vs. its associated service history for a given metallurgical condition, an exponential response is evident for events that are strongly affected by both temperature and time. Furthermore, if these events are considered as a function of T_m (as shown in Table 1) it is evident that, as the gamma prime size increases, the design temperature must also increase at an exponential rate. This discovery suggests some interesting kinetic mechanisms that should be further evaluated. And, at the same time, this breakthrough observation offers a more simplistic solution for what was previously an excessively complex estimate; i.e., where ogdoadicallydiced cubes or octodendrites are concerned.

Figure 12 and Table 2 define how this developed data can be used by manufacturing at turbine repair installations. A small blade sample is cut from a suspect blade and examined for the average D size using electron metallography at 5000× with the procedures that are described within this paper. For a given D (observed) value, it is easy to predict how much life is left for a properly evaluated blade specimen. For example, consider again Fig. 8, where a blade was retired because of "ears" and a D(observed) value of 0.7 μm. According to Fig. 12 and Table 2, that blade was retired prematurely since 37.5% life (L) was still remaining as determined by

$$(L) = [D(\max) - D(\text{obs})][D(\max) - D(\min)] \times 100,$$

where

$$(L) = [1.0 - 0.7][1.0 - 0.2] \times 100 = 37.5\%.$$

Usable blades are retired too often for business reasons and because technologists do not yet know how to properly predict life. This paper gives the turbine industry a new method for a reliable, reproducible way to safely evaluate retirement (R) or replacement (R′) or reuse (R″) where alloy 738 is concerned.

For this work, the severity (S) ratings averaged 13.7% which is classified as not significant since the limit boundary is assumed to be 15% maximum.

5. Conclusions

Most of the prominent findings have already been discussed in detail, but some additional points for alloy 738 do require an additional emphasis at this time.

(1) In the range of 0.3-0.6T_m, these rules hold: (A) interface controlled growth exists, (B) the gamma prime precipitate is coherent with its gamma matrix, (C) diffusion of interstital atoms occurs, and (D) useful life for a given gas turbine blade yet remains.

(2) In the range of 0.7-0.9T_m, these rules hold: (A) diffusion controlled growth applies, (B) the gamma prime precipitate is incoherent with its gamma matrix, (C) diffusion of substitutional atoms occurs, and (D) useful life approaches its terminal point for retirement (R) of previously used gas turbine blades.

References

1. C.G. Bieber and J.J. Galka, "Cast Nickel Base Alloy", Assigned to the International Nickel Company of New York, NY, USA Patent Number 3,619,182, Filed 1968 May, Patented 1971 Nov
2. L. Sheimbob and T. Cannon, EXTEX Ltd, Gilbert, AZ, Choice Alliance Dropping Cost of Parts and Maintenance in TR2 Terror Response Technology Report, *Aviation Today*, 2004
3. E. Lvov and D. Norsworthy, Influence of Service-Induced Microstructural Changes on the Aging Kinetics of Rejuvenated Nickel-based Superalloy Gas Turbine Blades, *J. Mater. Eng. Perform.*, 2001, **10**(3), p 299–312
4. E. Lvov, V.I. Levit, and M.J. Kaufman, Mechanism of Primary MC Carbide Deposition in Ni-base Superalloys, *Metallurgical and Materials Transactions A*, 2nd ed. (Materials Park, Ohio, USA), ASM International, 2004, **35A**, p 1669
5. C. Hays, Effects of {VIM + EBCHR} Refining for IN-738 Alloy, Journal of Materials Engineering and Performance, ASM International, Materials Park, Ohio, 44073-0002, USA, accepted
6. C. Hays, United States Patent Office, "Gas Turbine Blades By Means Other Than Casting," US60/879,448, Patent Pending, 2007 Jan
7. G. Petzow, Metallographic Etching, *Book*, 2nd ed. (Ohio), ASM International, Materials Park, USA, 1999, p 125
8. G.D. Preston, *The Diffraction of X-rays by Age Hardening Aluminum-Copper Alloys*, Proc. Royal Society, 1938, p 526
9. M. Durand-Charre, The Microstructure of Superalloys, *Book*, (London), CRC Press, 1997, p 72
10. T. Grosdidier, A. Hazotte, A. Simon, High Temperature $\gamma/\gamma + \gamma'$ Transformation in Single Crystal Ni-Based Superalloys, *Mater. Sci. Eng.*, 1998, **3**, p A256
11. S. Duval, S. Chambrelland, P. Caron, and D. Blayette, Phase Composition and Chemical Order in the Single Crystal Nickel Base Superalloy MC2, *Microsc., Microanal. Microstruc.*, 1994, **7**, p 65–84